Journal of Molecular Catalysis A: Chemical 302 (2009) 48–53

Contents lists available at ScienceDirect

Journal of Molecular Catalysis A: Chemical

journal homepage: www.elsevier.com/locate/molcata

The surface evolution of a catalyst jointly influenced by thermal spreading and solid-state reaction: A case study with an Fe_2O_3–MoO_3 system

Yan Huang[a,*], Liyan Cong[a], Jian Yu[a], Pierre Eloy[b], Patricio Ruiz[b]

[a] State Key Laboratory of Materials-oriented Chemical Engineering, College of Chemistry and Chemical Engineering, Nanjing University of Technology, Nanjing 210009, China
[b] Unite de Catalyse et Chimie des Matériaux Divisés, Université catholique de Louvain, B-1348 Louvain-la-Neuve, Belgium

ARTICLE INFO

Article history:
Received 18 June 2008
Received in revised form
25 November 2008
Accepted 26 November 2008
Available online 3 December 2008

Keywords:
Surface segregation
Thermal spreading
Iron oxide
Molybdenum oxide
X-ray photoelectron spectrum (XPS)
Methanol oxidation

ABSTRACT

The design and control of the surface is extremely important for the development of heterogeneous catalysts because surface properties always play a key role in catalytic performance. Therefore, it is of great interest to investigate the evolution of the surface state during the preparation of a catalyst. Mixed oxides are a particularly important group of catalytic materials. This work studied Fe_2O_3–MoO_3 as a model system, investigating the surface states jointly influenced by the thermal spreading of MoO_3 and the solid-state reaction that produces $Fe_2(MoO_4)_3$ during heat treatment. X-ray photo-electron spectroscopy, scanning electron microscopy and ^{57}Fe Mössbauer analysis were used to characterize the evolution of the surface and the bulk of solids, and the oxidation of methanol to formaldehyde was also used as a probe reaction. It was found that the evolution of the surface layer takes place mainly as follows: (i) a small amount of MoO_3 can be dispersed onto the surface of Fe_2O_3 via grinding; (ii) the thermal spreading of MoO_3 and the solid-state reaction start almost simultaneously at around 400 °C, leading to the coexistence of MoO_3 and $Fe_2(MoO_4)_3$ species on the surface of Fe_2O_3 grains; (iii) further thermal spreading and the solid-state reaction yield a shell of $Fe_2(MoO_4)_3$ encapsulating the remaining Fe_2O_3 grains, but a small amount of MoO_3 remains on the external surface of the resulting $Fe_2(MoO_4)_3$ shell; (iv) when the MoO_3 grains run out, the surface MoO_3 species also disappears.

1. Introduction

Mixed oxides are a particularly important group of catalytic materials. They can be conventionally prepared via solid-state reactions, which usually occur at the intergranular contacts of the reactant components. Sometimes, one component can spread spontaneously onto the surface of the other component along the contacting boundaries during heat treatment. This phenomenon is called "thermal spreading" or "solid-solid wetting" [1–5], and the driving force is the surface free energy. As a preferred means of mass transfer, thermal spreading greatly facilitates the solid-state reaction, and the reaction can take place on the entire surface of the stationary component, instead of at the intergranular contacts only. As a result, the remaining stationary component will be gradually encapsulated by the resulting new compound. Although phase analyses are almost routine in the study of mixed oxides, the information obtained may not directly relate to the catalytic results. It was well known that the surface, rather than the bulk, of a solid catalyst plays a key role in its catalytic performance [6]. Therefore, the surface design and its control are most important in catalyst development, and it is of great interest to investigate the evolution of the surface state during catalyst preparation.

Fe–Mo mixed oxides are well known catalysts for the oxidation of hydrocarbons and alcohols, particularly for the commercial oxidation of methanol to formaldehyde [7–13]. In the literature [1,4,14–18], the thermal spreading of MoO_3 has attracted considerable interest, being used as a "green" way to disperse MoO_3 on various supporting materials such as Al_2O_3, TiO_2, SiO_2, MgO, SnO_2 etc without generating waste gases or liquids. In these studies, the solid-state reaction, and particularly the surface evolution during preparation, has not usually been the main concern. This work studies the Fe_2O_3–MoO_3 mixture as a model system in order to investigate the evolution of the surface layer, which is jointly influenced by the thermal spreading of MoO_3 and the solid-state reaction giving $Fe_2(MoO_4)_3$. In addition to XPS, SEM and ^{57}Fe Mössbauer analyses, as a very sensitive surface analysis technique, the catalytic oxidation of methanol to formaldehyde was also employed as a probe for the surface analysis.

2. Experimental

Fe_2O_3 (AR, 99.95%) and MoO_3 (AR, 99.95%) with a molar ratio of 1:1 was ground mechanically, with some anhydrous ethanol added to help the grinding. After being dried at room temperature, the

* Corresponding author. Tel.: +86 25 83172253; fax: +86 25 83365813.
E-mail address: huangy@njut.edu.cn (Y. Huang).

1381-1169/$ – see front matter © 2008 Elsevier B.V. All rights reserved.
doi:10.1016/j.molcata.2008.11.033

mixture (denoted as "FeMo-RT") was divided into several parts to be treated at different temperatures. The resulting samples were denoted as FeMo-300, FeMo-400, FeMo-500 and FeMo-600, with heating temperatures of 300, 400, 500, and 600 °C, respectively. The calcination was done in air with a temperature ramp rate of 1.5 °C/min up to the target temperature, which was then maintained for 5 h. Higher heating temperatures were not used because of MoO_3 sublimation. For comparison with the effect of grinding, Fe_2O_3 and MoO_3 with the same ratio were also mixed by shaking violently in a glass bottle for 1 min, and the resulting mixture was denoted as "FeMo-SH".

The specific surface areas were measured with an ASAP 2020 Micromeritics analyzer using nitrogen adsorption at liquid nitrogen temperature. The degassing pre-treatment for each sample was done at 200 °C for 2 h. X-ray diffraction (XRD) analysis was conducted using a Siemens D8 Bruker-Axs III diffractometer with Cu-Kα radiation operating at 40 kV and 30 mA. A scanning electron microscopy (SEM) study was carried out with a QUANTA-2000 system. The ^{57}Fe Mössbauer analyses were performed using a VIS-1170-MO spectrometer with a 25 mCi ^{57}Co/Pd radiation source under constant acceleration mode, and the isomer shifts (IS) were referenced to α-Fe. The XPS analyses were performed with a Kratos Axis Ultra spectrometer (Kratos Analytical, Manchester, UK) equipped with a monochromatised aluminium X-ray source (powered at 10 mA and 15 kV). The sample powders were pressed into small stainless steel troughs mounted on a multi-specimen holder. The pressure in the analysis chamber was around 10^{-6} Pa. The hybrid lens magnification mode was used with the slot aperture, resulting in an analyzed area of 700 μm × 300 μm. The pass energy was set at 40 eV, and the charge stabilization was achieved with a Kratos Axis device. The energy resolution determined by the full width at half maximum (FWHM) of the Ag $3d_{5/2}$ peak was about 1.0 eV. The following sequence of spectra was recorded: survey spectrum, C 1s, O 1s, Fe 2p and Mo 3d. Finally, C 1s was recorded again to check the stability of charge compensation and the possible degradation of the samples during the analyses. The binding energies were referenced to 1s peak of adventitious carbon at 284.8 eV. The spectra were decomposed with a CasaXPS program (Casa Software Ltd., UK) with a Gaussian/Lorentzian (70%/30%) product function and after subtraction of a linear baseline. The XPS intensities were calculated using atomic sensitivity factors provided by the spectrometer manufacturer. Peak areas of Fe 2p (including Fe $2p_{1/2}$, Fe $2p_{3/2}$ and their shake-up peaks), Mo $3d_{5/2}$ and O 1s bands were used to quantify Fe, Mo and O.

Catalytic oxidation of methanol to formaldehyde was carried out in a fixed-bed quartz micro-reactor (i.d. 12 mm) operating at atmospheric pressure under continuous flow. The catalyst powders were pressed and sieved to 40–60 mesh, and 0.5 g catalyst was used each time after dilution with quartz grains (20–40 mesh) to 2 ml. A thermocouple was placed in the middle of the catalyst bed, and the void volume in the reactor was filled with quartz chips in order to avoid homogeneous reactions. The feed gas was formed by bubbling a mixture of nitrogen and oxygen through a methanol saturator, which was cooled with an ice-water bath. The flow rates of nitrogen, oxygen and the methanol vapor were 40.6, 7.5 and 1.9 ml/min. The catalytic reaction was performed at 260 °C, and the products were analyzed on-line by a Shimadzu GC-2014 gas chromatograph equipped with TCD and separation columns of Porapak-N and 5A Molecular Sieve.

3. Results

Apart from the original MoO_3 and Fe_2O_3, the $Fe_2(MoO_4)_3$ is the only new phase observed in FeMo-500 and FeMo-600 according to XRD analysis (JCDPS 31-642), and the MoO_3 phase almost disappears in FeMo-600. The ^{57}Fe Mössbauer analysis was also performed on FeMo-400, FeMo-500 and FeMo-600, and the results are exhibited in Fig. 1 and Table 1. Obviously, the spectra of FeMo-500 and FeMo-600 can be assigned to a sextet and doublet patterns, which must be assigned to α-Fe_2O_3 and $Fe_2(MoO_4)_3$, respectively [19]. A very weak peak can be recognized in the FeMo-400 spectra at the same position as $Fe_2(MoO_4)_3$, indicating that a small amount of $Fe_2(MoO_4)_3$ began to be formed in FeMo-400. The division of iron between Fe_2O_3 and $Fe_2(MoO_4)_3$ can be estimated by the corresponding relative areas listed in Table 1. About 14% of the source Fe_2O_3 has been converted in FeMo-500; the Fe_2O_3 conversion (ca. 28%) in FeMo-600 is close to the theoretical maximum (33%).

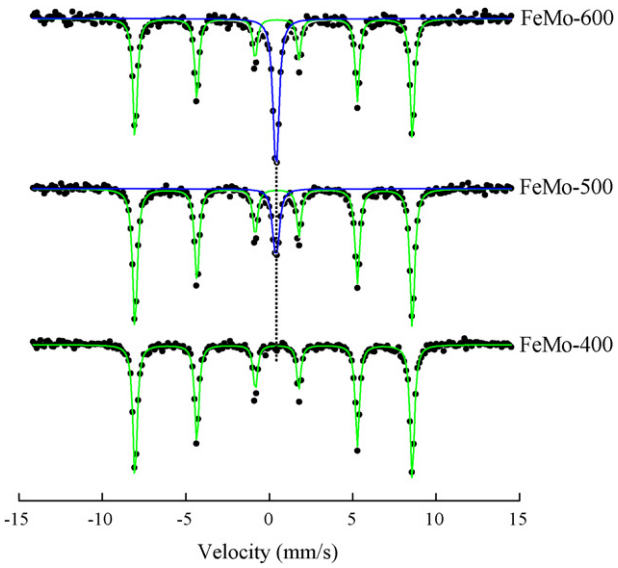

Fig. 1. Mössbauer spectra of Fe–Mo oxides.

XPS responses of all the samples can be ascribed to the elements Fe, O, Mo and the adventitious C; no other elements were detected. The binding energies (BE) of Mo $3d_{5/2}$, Fe $2p_{3/2}$ and O 1s are around 233, 711 and 530.5 eV, which can be assigned to Mo^{6+}, Fe^{3+} and O^{2-} species. No molybdenum species other than Mo^{6+} was observed. The Fe 2p bands are the characteristic signals of Fe^{3+}, which are composed of four peaks, i.e. Fe $2p_{3/2}$, Fe $2p_{1/2}$ and their shake-up peaks [20].

Fig. 2 compares the Mo 3d and Fe 2p bands between FeMo-SH and FeMo-RT. Both were mechanical mixtures of Fe_2O_3 and MoO_3, but the former was mixed by shaking and the latter by grinding. It was found that the Mo 3d band of FeMo-RT is significantly stronger than that of FeMo-SH. Fig. 3 compares the Fe 2p and Mo 3d spectra for FeMo-RT, FeMo-300, FeMo-400, FeMo-500 and FeMo-600. The intensity of Mo 3d for FeMo-500 was found to be the strongest, and the intensity of Fe 2p for FeMo-500 and FeMo-600 the weakest. The surface atomic ratio results are listed in Table 2, where $R_{Mo/Fe}$ and $R_{O/Fe}$ are denoted as the surface atomic ratio of Mo/Fe and O/Fe. The $R_{Mo/Fe}$ of FeMo-RT is larger than that of FeMo-SH, indicating that the grinding led to a dispersion of MoO_3 onto the Fe_2O_3 surface. The $R_{Mo/Fe}$ changed little for FeMo-300, slightly increased to 0.70 for FeMo-400, and sharply increased to 2.4 for FeMo-500, followed by a decrease to 1.7 for FeMo-600. A similar trend can be observed for $R_{O/Fe}$. According to the atomic ratios measured by XPS, the surface elemental concentrations of Mo, Fe and O can be calculated, and the results are demonstrated in Fig. 4. For reference, the nominal concentrations of these elements are shown with the dashed horizontal lines. It is observed that the surface concentrations of Mo are higher than the nominal ones, especially in the case of FeMo-500 and FeMo-600. The surface concentrations of Fe revealed the opposite situation. Significant deviations between the surface and

Table 1
Mössbauer results of Fe–Mo samples.

Sample	QS (mm/s)	IS (mm/s)	HF (kOe)	Line width (mm/s)	Relative area (%)
FeMo-400	0.20	0.37	515	0.30	>99
	–	0.41	–	–	<1
FeMo-500	0.21	0.37	514	0.33	86
	0.19	0.41	–	0.36	14
FeMo-600	0.20	0.37	515	0.29	72
	0.17	0.41	–	0.32	28

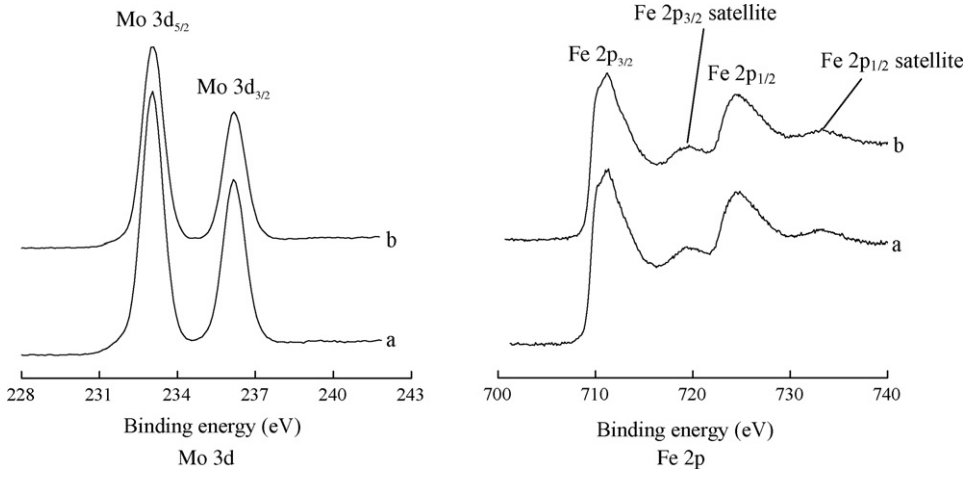

Fig. 2. Mo 3d and Fe 2p XPS spectra of (a) FeMo-RT and (b) FeMo-SH.

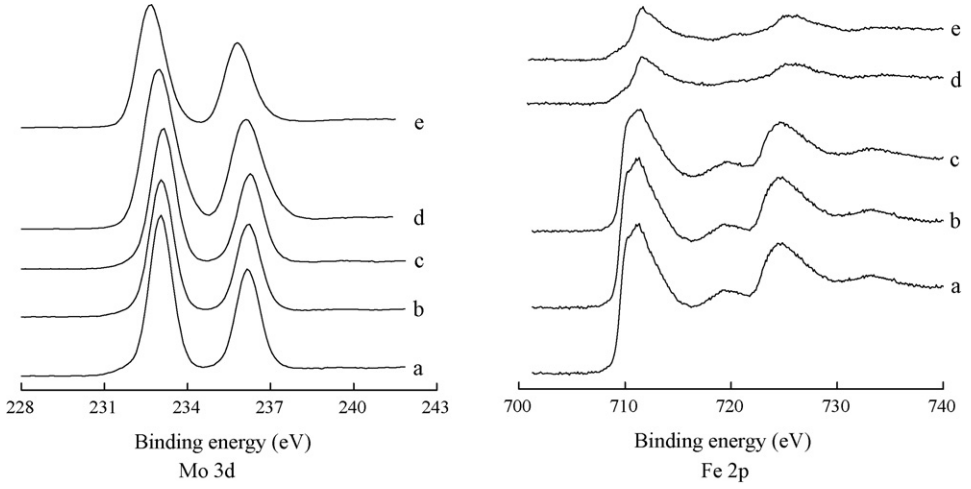

Fig. 3. Mo 3d and Fe 2p XPS spectra of (a) FeMo-RT, (b) FeMo-300, (c) FeMo-400, (d) FeMo-500, and (e) FeMo-600.

Table 2
Results of XPS.

Sample	$R_{Mo/Fe}$	$R_{O/Fe}$	FWHM of Mo $3d_{5/2}$ (eV)	Binding energy (eV)		
				Mo $3d_{5/2}$	Fe $2p_{3/2}$	O 1s
FeMo-SH	0.45	2.7	1.02	233.1	710.8	530.5
FeMo-RT	0.60	3.2	0.99	233.0	710.7	530.4
FeMo-300	0.58	3.1	1.02	233.1	710.8	530.5
FeMo-400	0.70	3.4	1.09	233.1	710.8	530.6
FeMo-500	2.4	7.4	1.34	233.0	711.8	530.7
FeMo-600	1.7	5.7	1.15	232.7	711.8	530.6

$R_{Mo/Fe}$ and $R_{O/Fe}$ are the atomic ratio of Mo/Fe and O/Fe measured by XPS.

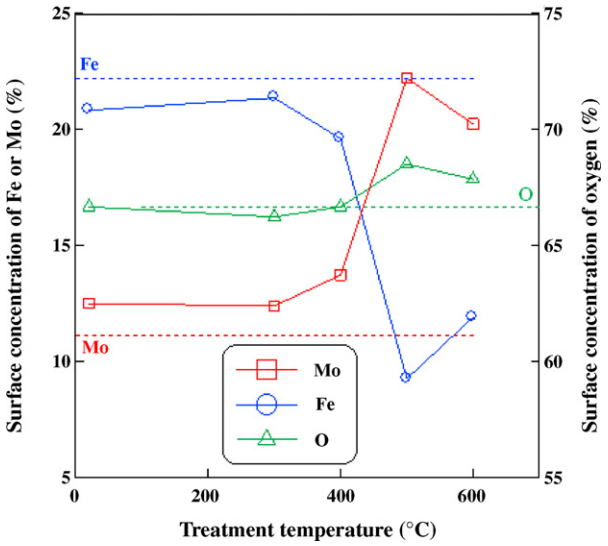

Fig. 4. Effect of the treatment temperature on the atomic surface concentrations of Mo, Fe and O.

nominal oxygen concentrations were only observed with FeMo-500 and FeMo-600.

SEM micrographs are shown in Fig. 5. The Fe_2O_3 component presents fine grains, and the original MoO_3 as-purchased was flake-like crystals, which can be broken into strip-like pieces and powders via grinding. No significant differences can be observed between the FeMo-RT, FeMo-300 and FeMo-400 samples. In FeMo-500, the MoO_3 strips look spindle-shaped, as if partially melted, and accordingly the "Fe_2O_3" grains became larger. In FeMo-600, most of the MoO_3 grains disappeared and the "Fe_2O_3" grains grew further.

Catalytic oxidation of methanol was carried out at 260 °C. The HCHO and H_2O were the only products detected over all the catalysts Therefore, the conversion of methanol or the yield of HCHO can be used to denote the catalytic activity of each catalyst. For comparison with FeMo-300, pure Fe_2O_3 and pure MoO_3 were also tested after a heat treatment at 300 °C for 5 h. It was found in Table 3 that pure MoO_3 and pure Fe_2O_3 are almost inactive (the corresponding methanol conversions are only 4.6% and 3.7%); while FeMo-300 is highly active (the methanol conversion reaches 71.3%). Table 3 also indicates that FeMo-400 is the most active catalyst in this work. A significant decrease in activity was observed for FeMo-500, and the activity of FeMo-600 was further reduced, down to even less than half that of FeMo-500.

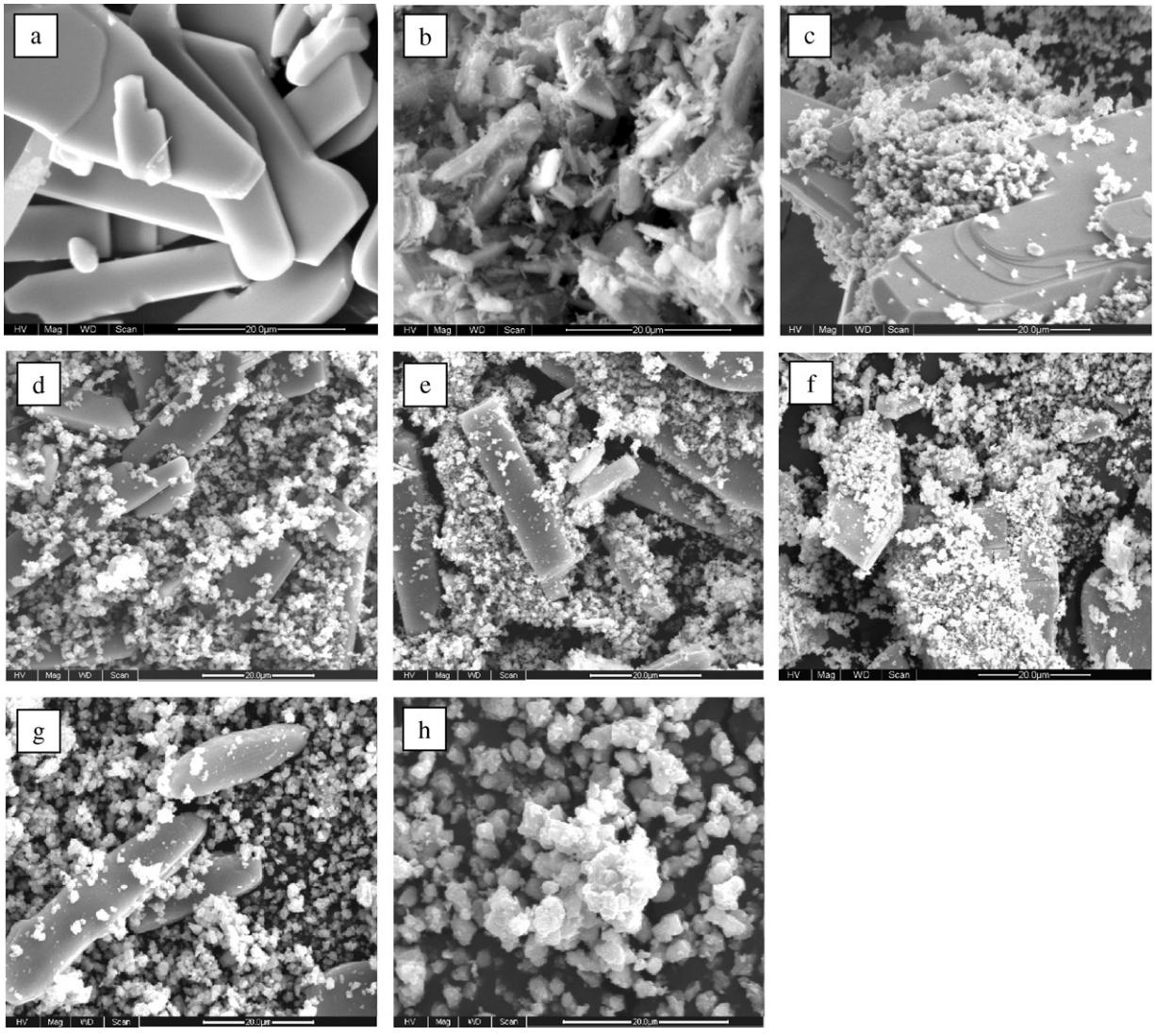

Fig. 5. SEM micrographs of (a) MoO_3 as purchased, (b) MoO_3 after grinding, (c) FeMo-SH, (d) FeMo-RT, (e) FeMo-300, (f) FeMo-400, (g) FeMo-500, and (h) FeMo-600.

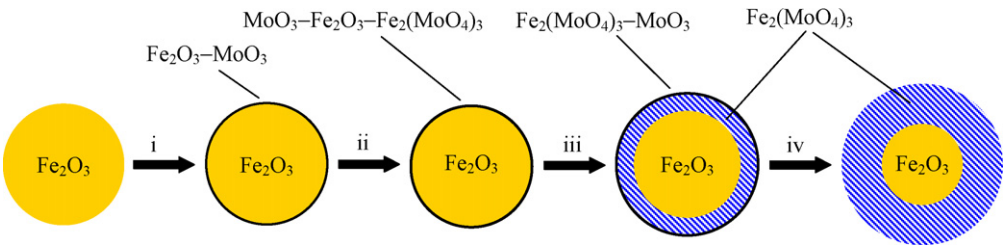

Fig. 6. Scheme of the surface evolution starting with Fe_2O_3 grains in a mixture of Fe_2O_3:MoO_3 = 1:1 (mol/mol).

4. Discussion

During grinding, the softer grains can be pulverized and some of them may be dispersed onto the surface of other grains [20,21]. Therefore, it is not surprising that some MoO_3 can be dispersed onto the Fe_2O_3 surface during grinding and that the $R_{Mo/Fe}$ of FeMo-RT measured by XPS is higher than that of FeMo-SH. As shown in Table 3, the FeMo-300 catalyst, which is composed of MoO_3 and Fe_2O_3 phases, is much more active than any of its two components. This may be attributed to the formation of an active layer on the Fe_2O_3 surface, where some MoO_3 presents. For example, there can be a diffusion of Mo^{6+} into the Fe_2O_3 surface [22].

An increase in the heating temperature from 300 to 400 °C leads to an increase in $R_{Mo/Fe}$ from 0.58 to 0.70, indicating that more MoO_3 has been dispersed onto Fe_2O_3 surface. Meanwhile, a very small amount of $Fe_2(MoO_4)_3$ began to be formed, preferably, on the Fe_2O_3 surface. Most likely, the surface layer of Fe_2O_3 grains in FeMo-400 could be composed of: (i) $Fe_2(MoO_4)_3$, (ii) $Fe_2(MoO_4)_3$–MoO_3, (iii) $Fe_2(MoO_4)_3$–Fe_2O_3, or (iv) $Fe_2(MoO_4)_3$–MoO_3–Fe_2O_3. Since the $R_{Mo/Fe}$ of FeMo-400 measured by XPS is only 0.70, the cases (i) and (ii) must be excluded, otherwise the $R_{Mo/Fe}$ of FeMo-400 will be beyond 1.5 (i.e. the nominal Mo/Fe ratio in $Fe_2(MoO_4)_3$).

Further increase in the treatment temperature promoted both the thermal spreading of MoO_3 and the solid-state reaction, and the cooperation of these two processes gradually builds up a shell of $Fe_2(MoO_4)_3$ on the remaining Fe_2O_3 grains. Such a model of the formation of $Fe_2(MoO_4)_3$ shell on Fe_2O_3 surface has been reported by House et al. [23,24]. As indicated by Mössbauer results, about 14% of Fe_2O_3 and the consequent 42% of MoO_3 have been transformed in FeMo-500. In this case, the surface of the $Fe_2(MoO_4)_3$ shells will be composed of "$Fe_2(MoO_4)_3$" or "$Fe_2(MoO_4)_3$–MoO_3". The $R_{Mo/Fe}$ of FeMo-500 has been increased by a factor of up to 2.4, but it is still not too far from the nominal atomic ratio of Mo/Fe in $Fe_2(MoO_4)_3$, indicating that the concentration of excessive MoO_3 on the $Fe_2(MoO_4)_3$ shells cannot be high, namely, the rate of the MoO_3 spreading is close to the rate of MoO_3 consumption by the reaction.

With the running out of the MoO_3 component, the thermal spreading of MoO_3 or the formation of $Fe_2(MoO_4)_3$ would not develop anymore, leaving the remaining Fe_2O_3 grains encapsulated by a thick shell of $Fe_2(MoO_4)_3$. Accordingly, the $R_{Mo/Fe}$ of FeMo-600 measured by XPS is 1.7, which is very close to the nominal atomic ratio of Mo/Fe in $Fe_2(MoO_4)_3$. Moreover, Fig. 4 indicates that the surface elemental concentrations of Mo, Fe and O measured by XPS are 20%, 12% and 68%, respectively, which are almost the same as those in $Fe_2(MoO_4)_3$: 18%, 12% and 70%.

Fe–Mo mixed oxides have been intensively studied as catalysts for the oxidation of methanol to formaldehyde, and it was well established that $Fe_2(MoO_4)_3$ is not active unless enriched by MoO_3 on its surface [8,11,25]. That is, a surface layer composed of "$Fe_2(MoO_4)_3$" or "$Fe_2(MoO_4)_3$–Fe_2O_3" is not active. This makes the probe reaction a powerful technique for surface analysis. Indeed, Table 3 indicates that FeMo-600 is much less active than other Fe–Mo catalysts. As discussed above, the surface layer of the Fe_2O_3 grains in FeMo-400 is possibly composed of (i) "$Fe_2(MoO_4)_3$–Fe_2O_3" or (ii) "$Fe_2(MoO_4)_3$–MoO_3–Fe_2O_3", and the surface layer of the $Fe_2(MoO_4)_3$ shells in FeMo-500 is possibly composed of (i) "$Fe_2(MoO_4)_3$" or (ii) "$Fe_2(MoO_4)_3$–MoO_3". Now, the possibility (i) for both catalysts should be excluded because the activities of FeMo-400 and FeMo-500 are more than twice that of FeMo-600. Although the surface layers composed of "Fe_2O_3–MoO_3" and especially of "Fe_2O_3–$Fe_2(MoO_4)_3$–MoO_3" were found to be highly active, they are simply an intermediate state and their relatively low stability may limit any industrial feasibility.

Table 3
Catalytic activities of the catalysts for selective methanol oxidation.

Catalysts	Surface area (m^2/g)	Methanol conversion (%)
Fe_2O_3	4.14	3.7
MoO_3	1.27	4.6
FeMo-300	2.25	71.3
FeMo-400	2.17	75.3
FeMo-500	1.25	62.5
FeMo-600	1.31	29.1

5. Conclusion

A mixture with Fe_2O_3:MoO_3 = 1:1 was studied as a model catalytic system. The state of the surface layer on the Fe_2O_3 grains during heat treatment was jointly influenced by the thermal spreading of MoO_3 and the solid-state reaction. The surface evolution can be illustrated in Fig. 6:

(i) A small amount of MoO_3 can be dispersed onto the surface of Fe_2O_3 via grinding;
(ii) The thermal spreading of MoO_3 and the solid-state reaction start almost simultaneously at around 400 °C, leading to the coexistence of MoO_3 and $Fe_2(MoO_4)_3$ species on the surface of Fe_2O_3 grains;
(iii) Further thermal spreading and solid-state reaction yield a shell of $Fe_2(MoO_4)_3$ encapsulating the remaining Fe_2O_3 grains, but a small amount of MoO_3 remains on the surface of the resulting $Fe_2(MoO_4)_3$ shell;
(iv) When the MoO_3 grains run out, the surface MoO_3 species also disappears.

Acknowledgements

Dr. Y. Huang thanks the financial supports by Natural Science Foundation of China (NSFC, No. 20576055 and No. 20876075) and Program for Changjiang Scholars and Innovative Research Team in University (No. IRT0732).

References

[1] H. Knözinger, E. Taglauer, in: J.J. Spivey, S.K. Agarwal (Eds.), Catalysis, vol. 10, The Royal Society of Chemistry, Cambridge, 1993, p. 1.
[2] Y. Xie, Y. Tang, Adv. Catal. 37 (1990) 1.

[3] Y. Huang, G. Wang, R.X. Valenzuela, V.C. Corberán, Appl. Surf. Sci. 210 (2003) 346.
[4] S. Braun, L.G. Appel, V.L. Camorim, M. Schmal, J. Phys. Chem. B 104 (2000) 6584.
[5] J. Haber, T. Machej, E. Servicka, I. Wachs, Catal. Lett. 32 (1995) 101.
[6] Y. Huang, P. Ruiz, Appl. Surf. Sci. 252 (2006) 7849.
[7] W. Kuang, Y. Fan, Y. Chen, Langmuir 16 (2000) 5205.
[8] F. Trifirò, M. Carbucicchio, P.L. Villa, Hyperfine Interact. 111 (1998) 17.
[9] V. Diakov, A. Varma, Chem. Eng. Sci. 58 (2003) 801.
[10] S.A.R.K. Deshmukh, M.A. van Sint, J.A.M. Kuipers, Appl. Catal. 289 (2005) 240.
[11] A.P.V. Soares, M.F. Portela, A. Kiennemann, L. Hilaire, J.M.M. Millet, Appl. Catal. 206 (2001) 221.
[12] M.P. House, A.F. Carley, M. Bowker, J. Catal. 252 (2007) 88.
[13] A. Andersson, M. Hernelind, O. Augustsson, Catal. Today 112 (2006) 40.
[14] Y. Cai, C. Wang, I.E. Wachs, Stud. Surf. Sci. Catal. 110 (1997) 255.
[15] J. Handzlik, J. Ogonowski, J. Stoch, M. Mikołajczyk, P. Michorczyk, Appl. Catal. 312 (2006) 213.
[16] S.R. Bare, Langmuir 14 (1998) 1500.
[17] G.K. Mestl, T.K.K. Srinivasan, Catal. Rev. 40 (1998) 451.
[18] S.R. Stampf, Y. Chen, J.A. Dumesic, C. Niu, C.G. Hill Jr., J. Catal. 105 (1987) 445.
[19] D.D. Radev, V. Blaskov, D. Klissurski, I. Mitov, A. Toneva, J. Alloys Compd. 256 (1997) 108.
[20] Y. Huang, P. Ruiz, J. Phys. Chem. B 109 (2005) 22420.
[21] B. Pillep, P. Behrens, U. Schubert, J. Spengler, H. Knözinger, J. Phys. Chem. B 103 (1999) 9595.
[22] L. Dong, K. Chen, Y. Chen, J. Solid State Chem. 129 (1997) 30.
[23] M.P. House, Ph.D. Thesis, Cardiff University, 2007.
[24] M.P. House, A.F. Carley, R. Echeverria-Valda, M. Bowker, J. Phys. Chem. C 112 (2008) 4333.
[25] M.R. Sun-Kou, S. Mendioroz, J.L.G. Fierro, J.M. Palacios, A. Guerrero-Ruiz, J. Mater. Sci. 30 (1995) 496.